Available online at www.sciencedirect.com
ScienceDirect
Remote Sensing of Environment 112 (2008) 934–938
Remote Sensing of Environment
www.elsevier.com/locate/rse

Practical application of the "turbid water" flag in ocean color imagery: Interference with sun-glint contaminated pixels in open ocean

André Morel *, Bernard Gentili

Laboratoire d'Océanographie de Villefranche (CNRS-INSU and Université P. & M. Curie), BP 08, 06238 Villefranche-sur-mer, France

Received 2 May 2007; received in revised form 4 July 2007; accepted 4 July 2007

Abstract

A simple method to identify turbid, sediment-loaded, waters within satellite ocean color imageries was recently proposed (A. Morel and S. Bélanger, Remote Sensing of Environment, 102, (2006), 237–249). Systematic application of this method to the level-3 composites obtained from three ocean color sensors shows that the "turbid" flag is often raised in the open ocean, especially in the sub-tropical oligotrophic gyres, where turbidity is unlikely. In addition these flagged zones migrate with season, and clearly follow the sun declination course. The combination of low chlorophyll waters with a residual sun-glint is at the origin of this artifact. Simple approaches for eliminating such a misleading detection are proposed. The identification and elimination of the bias are also needed in particular for an unambiguous detection of the presence of calcite (coccolithophores) in open waters.

Keywords: Ocean color; Turbidity threshold; Open ocean; Interference turbidity vs sun-glint

1. Motivation: existence of an interference

In a recent paper (Morel & Bélanger, 2006, hereafter denoted MB06), an improved technique was proposed to detect "turbid" waters within satellite color imageries. It is simply based on the enhancement of irradiance reflectance, R, in the green part of the spectrum resulting from the presence of sediments in suspension. This presence is essentially expected in coastal zones where mineral particles may be brought to the sea by rivers; even in the absence of such riverine outflow, sediments may be resuspended from the bottom under the influence of waves and tides in sufficiently shallow waters. In deep, open ocean, Case 1 waters, far from such potential sources of sediment, no enhancement of reflectance is expected, except in particular circumstances. These exceptions include the occurrence of highly reflecting phytoplanktonic populations (coccolithophores and detached calcite liths, or species with gas vacuoles), or the presence of abundant bubbles and foam.

The proposed detection tool makes use of a reflectance threshold, $R_{\mathrm{lim}}([\mathrm{Chl}], \theta_s)$, which varies with the chlorophyll concentration, [Chl], and also depends on the observational conditions, essentially on the zenith-sun angle, θ_s. In the discussion (point 1 in MB06), it was stressed that an insufficient rejection of areas contaminated by residual sun-glint may lead to a raising of the "turbid flag" in zones where such a turbidity is unlikely or at least suspect.

Actually, this drawback was not frequently detected (or not identified as such) when studying coastal zones influenced by river discharges and sediment resuspension. More systematic examinations, however, extended beyond the coastal zones and encompassing the global ocean, have shown that the turbidity flag was rather frequently and questionably raised in open ocean. When considering the level-3 data for the whole ocean, this raising occurs essentially within the oligotrophic belts around the planet (roughly within the 15–30° North and South zonal bands), where [Chl] is generally below ~0.15 mg m^{-3}. The relative excess of irradiance reflectance, ΔR, in the green part of the spectrum (with $\lambda = 560$, 555, or 551 nm) is defined as the quantity (Eq. (14) in MB06)

$$\Delta R(\lambda) = (R(\lambda) - R_{\mathrm{lim}}(\lambda))/R_{\mathrm{lim}}(\lambda)$$

where $R(\lambda)$, expressed as %, is $R(\lambda, \theta_s = 0)$ in the case of level-3 data (because these data are exactly normalized products), so that R_{lim} takes its particular value, namely $R_{\mathrm{lim}}(\lambda,[\mathrm{Chl}], \theta_s = 0)$.

* Corresponding author.
E-mail address: morel@obs-vlfr.fr (A. Morel).

0034-4257/$ - see front matter © 2008 Published by Elsevier Inc.
doi:10.1016/j.rse.2007.07.009

This ΔR excess detected in the sub-tropical zones remains low (generally <20% of the R_{lim} value); yet it is significant and especially surprising.

Furthermore, a seasonal migration of the "flagged" zones is apparent. They are located in the northern hemisphere in June–July, in the southern hemisphere in December, and are symmetrically placed on both sides of the Equator in March and September. During the equinoctial period, the flag is not raised along the Equator itself, where generally [Chl] experiences a maximum compared to values within the sub-tropical gyres. Examples showing monthly level-3 composites from the three sensors are provided in the four plates of Fig. 1A (the raising of the flag appears equally when the ΔR test is applied to daily, weekly or monthly composites). The zonal (and seasonal) migration of the flagged zones is ostensibly in keeping with sun's declination, as demonstrated by the density plots shown in Fig. 1B. This observation suggests an effect of the sun-glint.

Despite the fact that SeaWiFS is provided with a tilting capability, whereas MERIS and MODIS-A instruments are not tilted, the same phenomenon (presumably an artifact) is present in the three imageries. Its intensity is varying; SeaWiFS and MERIS imageries exhibit similar patterns, albeit accentuated in MERIS; the effect is less intense in the MODIS-A L3 products, since the maximal ΔR values, close to zero, often remain slightly negative. The varying intensities are likely related to the sun-glint rejection criteria adopted when producing the level-3 maps, which is beyond the scope of the present paper.

Rather, the question is then: why is this effect particularly marked in the sub-tropical oligotrophic gyres, where [Chl] is at its minimum?

2. Analysis: the cause of the interference

The answer actually is contained in Figs. 4a and b of the MB06 paper. In the domain of low [Chl] (say below 0.2 mg m^{-3}), the field data for Case 1 waters are closely bordering upon the modeled reflectance curves, R_{lim} (θ_s, [Chl]), which were adopted as upper limits, and used as thresholds. As a consequence, a small excess of radiance $\Delta R(\lambda)$ due to uncorrected glint can easily trigger the flag, whereas in the other part of the [Chl] range (>0.2 mg m^{-3}), the risk is less marked, to the extent that the adopted threshold is distinctly above the Case 1 non-turbid field data.

Applying more stringent rules to eliminate those pixels contaminated by weak residual sun-glint signals could be a possible solution during the data processing. The drawback with such a solution, however, does exist that some pixels which are acceptable for other applications (e.g., for the retrieval of [Chl]), will be ignored in the subsequent processing. Therefore, if the elimination of contaminated pixels is not envisaged, it is necessary to eliminate the consequences of such interferences.

3. Elimination of the interference

More realistically, a limited raising of the (unintentionally too severe) threshold appears preferable. In practice, and somewhat arbitrarily, this can be effected by adding a small constant to R_{lim}, whatever [Chl]. Doing so, the impact is essentially at low [Chl], when $R_{lim}(\lambda)$ is small, while it progressively diminishes at moderate or high [Chl], when R_{lim} increases (Fig. 2). Tentatively, the addition to R_{lim} of an arbitrary constant (equal to 0.27%, adjusted by trials and errors) eliminates totally the wrongly detected turbid pixels within the oligotrophic gyres in the SeaWiFS and MODIS-A imageries. Yet, a few contaminated pixels (about 0.1% of the total number of pixels) may sporadically remain in MERIS imagery (they disappear if the arbitrary constant is set equal to 0.35%). Perhaps the present "medium glint mask" that is applied before producing the MERIS level-3 would not be severe enough; but these scattered contaminated pixels may as well result from noise.

An even simpler solution, however, is equally efficient for the three sensors and scientifically more justifiable. It consists of realizing that if [Chl] has been found to be <0.2 mg m^{-3}, i.e., if "blue" waters have been clearly identified, then they cannot be affected by the presence of sediments. Indeed, waters with low [Chl] but with high sediment content, or as well coccolithophores, appear turquoise (bright blue-green color); the color shift mainly results from the reduction of the "penetration depth" (Gordon & McCluney, 1975), due to the increased backscattering. As a consequence, these bright waters, with their enhanced reflectivity in the green, are wrongly interpreted by standard (band ratio) algorithms as containing a substantial amount of chlorophyll. Therefore, a high blue-to-green ratio, leading to low [Chl], is in no way compatible with a significant turbidity; consequently, trying to apply the detection tool in such zones is definitely not needed. Actually, this method and the previous one (heightening the threshold) essentially provide the same results; in the case of MERIS however, the few pixels that remained flagged as turbid inside the oligotrophic gyres, when the constant added to R_{lim} is 0.27%, totally vanish when the criterion based on [Chl] is operated.

Examples of application of both methods are provided in Fig. 1C. As expected, the flag logically remains raised where it must be, namely in many coastal or shallow waters and inside river plumes (admittedly, the maps in Fig. 1 must be enlarged to visualize these zones, but see Figs. 6 and 8 in MB06). The flag is also raised in some rather wide zones, as for instance, the Yellow Sea, the Indonesian Seas, the Gulf of Carpentaria, or the Bahamas banks, i.e., in zones already known for their high and more or less permanent turbidity (or reflecting bottoms in banks). It is still raised in some remote oceanic areas, outside of the sub-tropical gyres; and such features which are not related to the misleading glint must have physical meanings, as briefly summarized below.

4. Facts and artifacts

It is beyond the scope of the present study to analyze the oceanographic and biogeochemical causes of such open ocean "turbidity" (in the sense defined here, i.e., excess of reflectance in the green), which episodically appears in some oceanic zones outside of the sun-glint contaminated areas. The intent here is just to point out some of the main features observed in the three imageries.

In the Northern hemisphere, large patches of reflective waters occur during the boreal summer. They extend from the British Islands toward Iceland, Greenland, and Nova Scotian shelf, and are very likely related to the presence of coccolithophores (Holligan et al., 1993; Brown & Yoder, 1994; Balch et al., 2005 and references herein). The same phenomenon intensely occurs

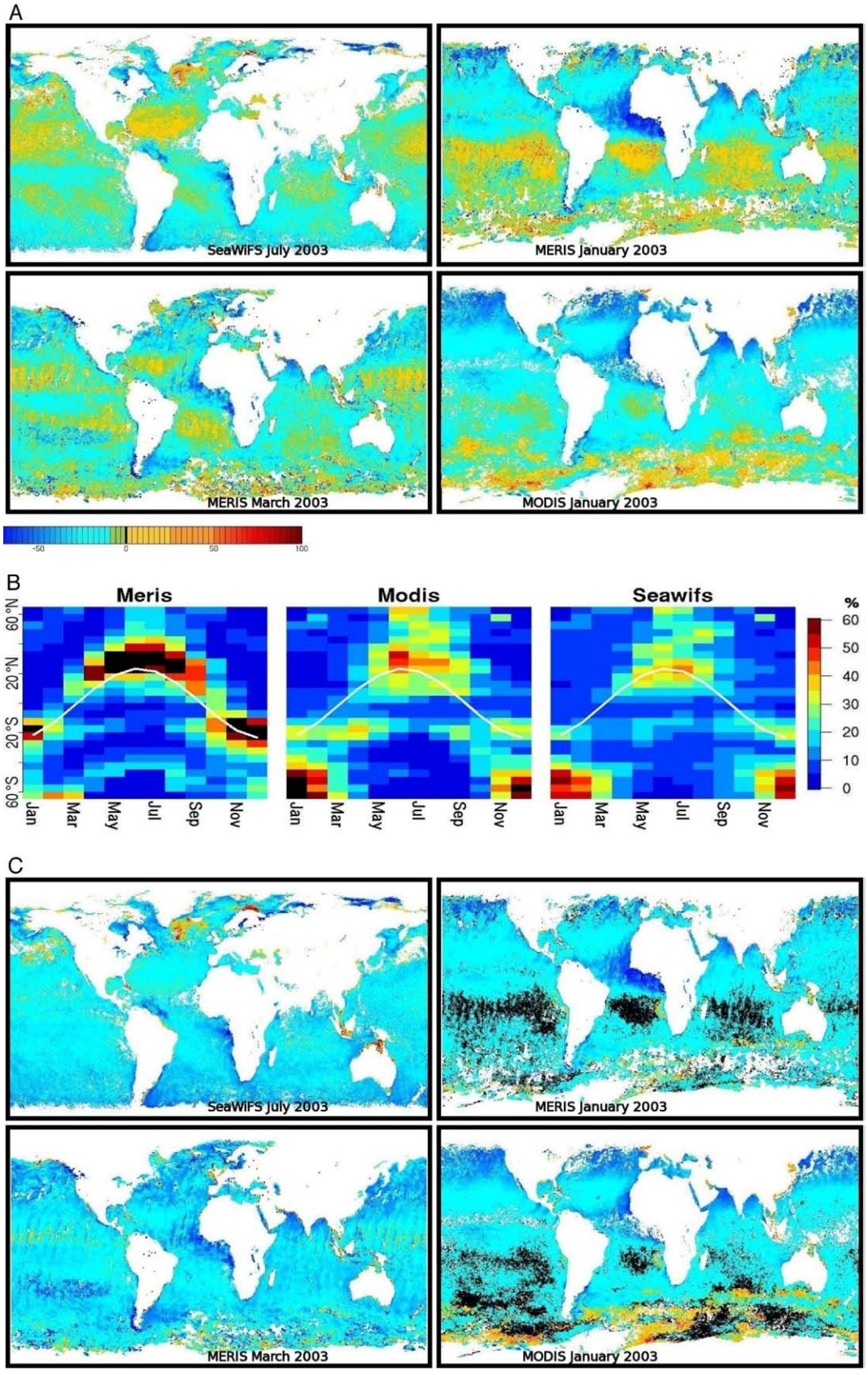

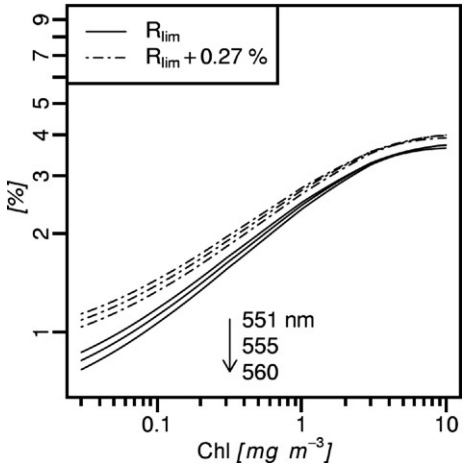

Fig. 2. As a function of the chlorophyll concentration, variations of $R_{lim}(\lambda,[Chl], \theta_s=0)$, expressed as percent, and for the three wavelengths 551, 555, and 560 nm (from top to bottom) as computed for application to the MODIS-A, SeaWiFS, and MERIS data, respectively. The effect of the addition to the theoretical thresholds R_{lim} of a constant equal to 0.27% is also shown (dashed curve) for each wavelength.

in July–August in the Barents Sea around the North Cape (Smyth et al., 2004), whereas in the southern part of the Gulf of Alaska, similar features are detected in April–May.

In the Southern Ocean, an almost continuous belt of reflective waters, encircling the Antarctic continent, appears during the austral summer, with a maximum in January; the color plates 5a and 5d (in Balch et al., 2005) show the same phenomenon. The presence within this Antarctic Polar Front Zone of algae with apparently particular optical properties (e.g., Mitchell & Holm-Hansen, 1991; Eiras Garcia et al., 2005) may explain this high reflectance, mainly as a result of the enhanced particle backscattering efficiency (Reynolds et al., 2001). The enhancement of reflectance due to the presence of foam in this zone where high winds prevail is likely to be also considered.

When examining individual scenes at a regional scale, excessive reflectance can be locally detected over a few pixels; yet, an interpretation in terms of turbidity is highly dubious. These anomalous pixels mostly result from the influence of well known adjacency effects (see e.g. Lyapustin & Kaufman, 2001). As such, they are easily identifiable along bright coasts, or in the vicinity of clouds. Even for monthly level-3 products, high levels of cloud cover reduces the number of pixels available for compositing, and the remaining pixels may be contaminated by nearby clouds and cloud shadows (this artifact cannot be excluded in the Southern Ocean within the 50°–60°S zonal band— see, e.g., MERIS and MODIS-A maps for January in Fig. 1). Imperfect atmospheric correction could also be at the origin of a misplaced flag. Indeed, the marine signal in the green part of the spectrum is weak in low chlorophyll waters, and thus sensitive to a slight underestimate of the atmospheric signal. It is difficult to assess the importance of this effect, which is also a possibility when the adjacency effect seems improbable.

5. Conclusion

It is worth emphasizing that the initial targeted objective of the turbidity flag was a quantified description of phenomena associated with shallow water, river plumes and sediment transport in coastal environment and shelves. This aim remains unchanged.

Somewhat surprisingly, however, this flag, with its corollary, namely the quantified excess of reflectance (or radiance), is sensitive enough to put in evidence in the open ocean zones where the "apparent" turbidity actually results from the residual presence of sun-glint contaminated pixels; these pixels, with admittedly a weak contamination, have passed the rejection screening processes. The elimination of this artifact can be easily performed. It is needed to remove the ambiguity between residual glint and really turbid waters that may occur in the open ocean; indeed, such occurrences most often correspond to the presence offshore of coccolithophores. Provided that the ambiguity has been removed, the excess of radiance is an efficient tool to delineate coccolithophores blooms. It is not essentially differing from other methods and specific algorithms as those proposed for MODIS by Balch et al. (2005). The present tool, however, is straightforward as it rests on a single band information associated with an already available product, i.e., the chlorophyll concentration. The identification of glint contaminated water-leaving radiances is also needed when the interpretation of the ocean color data partly or totally relies on the magnitude of the marine signals, and not on their ratios, as for instance the experimental algorithm for calcite (Balch et al., 2005).

Fig. 1. A) Application of the turbid flag to monthly level-3 composites obtained from the three ocean color sensors as indicated (4320×2160 pixels for SeaWiFS and MODIS, 9×9 km bins for MERIS); the months represented correspond to the two solstices and the vernal equinox (Year 2003). As the radiances used when building the L-3 composites are exactly normalized radiances, the threshold is $R_{lim}([Chl], \lambda, \theta_s=0)$ (see Fig. 2).The color scale quantifies $\Delta R(\lambda)$ as percent, and the green color corresponds to $\Delta R(\lambda)$ values between −10% and 0% and is used for the pixels which are just below R_{lim}. Patterns similar to those found for MERIS and SeaWiFS in sub-tropical areas also exist in MODIS imagery but they are less contrasted, with ΔR values just below 0 (in green). B) Again for the year 2003 and the three sensors, density plots (color scale) of the percent of oceanic area where ΔR is positive (MERIS and SeaWiFS), (or $\Delta R > -10\%$, for MODIS), as a function of latitude (ordinates from 60°S to 60°N), and months (abscissae from January to December). The declination of the sun is also displayed as the white curves. Note also the importance of the flagged zones in austral summer near the Antarctic continent (discussed in the text). C) In reference to panels in A, examples of elimination of the sun-glint artifact by two methods, either by heightening the threshold (SeaWiFS, July or MERIS, March; left column) or by identifying the pixels with $\Delta R > 0$, when [Chl] is <0.2 mg m^{-3} (MERIS, January), or again when [Chl] is <0.2 mg m^{-3}, and $\Delta R > -10\%$ (MODIS-A January). In these two latter images (right column), when the flag is disabled, the identified pixels are shown as black pixels. Note that there are not too many "black" pixels in the Southern Ocean, which means that the detected turbidity is not a sun-glint artifact. Notice also that there are more clouds (or more rejected pixels at the issue of the processing, or unseen pixels) in the MERIS imagery than in the MODIS imagery. (For interpretation of the references to color in this figure legend, the reader is referred to the web version of this article.)

Acknowledgements

We are indebted to Yannick Huot for helpful discussions on an early draft of this paper, and we thank the anonymous reviewers for their helpful comments on the original manuscript.

References

Balch, W. M., Gordon, H. R., Bowler, B. C., Drapeau, D. T., & Booth, E. S. (2005). Calcium carbonate measurements in the surface global ocean based on Moderate Resolution Imaging Spectroradiometer data. *Journal of Gephysical Research*, *110*, C07001. doi:10.1029/2004JC002560

Brown, C. W., & Yoder, J. A. (1994). Coccolithophorid blooms in the global ocean. *Journal of Geophysical Research*, *99*, 7467−7482.

Eiras Garcia, C. A., Tavano Garcia, V. M., & McClain, C. R. (2005). Evaluation of SeaWiFS chlorophyll algorithms in the South western Atlantic and Southern Oceans. *Remote Sensing of Environment*, *95*, 125−137.

Gordon, H. R., & McCluney, W. R. (1975). Estimation of the depth of sunlight penetration in the sea for remote sensing. *Applied Optics*, *14*, 413−416.

Holligan, P. M., Fernandez, E., Aiken, J., Balch, W. M., Boyd, P., Burkill, P. H., et al. (1993). A biogeochemical study of the coccolithophore, *Emiliania huxleyi*, in the North Atlantic. *Global Biogeochemical Cycles*, *7*(4), 879−900.

Lyapustin, A. I., & Kaufman, Y. F. (2001). Role of adjacency effect on the remote sensing of aerosol. *Journal of Geophysical Research*, *106*, 11909−11916.

Mitchell, B. G., & Holm-Hansen, O. (1991). Bio-optical properties of Antarctic Peninsula waters: Differentiation from temperate ocean models. *Deep-Sea Research*, *38*, 1009−1028.

Morel, A., & Bélanger, S. (2006). Improved detection of turbid waters from ocean color sensors information. *Remote Sensing of Environment*, *102*, 237−249.

Reynolds, R. A., Stramski, D., & Mitchell, B. G. (2001). A chlorophyll-dependent semianalytical reflectance model derived from field measurements of absorption and backscattering coefficients within Southern Ocean. *Journal of Geophysical Research*, *106*, 7125−7138.

Smyth, T. J., Tyrell, T., & Tarrant, B. (2004). Time series of coccolithophores activity in the Barentz Sea, from twenty years of satellite imagery. *Geophysical Research Letters*, *31*, L11302. doi:10.1029/2004GL019735.2004